DOI: 10.1002/ange.200802815

Redox Chemistry

Structure and Redox Activity of Copper Sites Isolated in a Nanoporous P4VP Polymeric Matrix**

Elena Groppo, Mohammed Jasim Uddin, Silvia Bordiga, Adriano Zecchina, and Carlo Lamberti**

Dedicated to the Catalysis Society of Japan on the occasion of its 50th anniversary

In the recent years, metal-containing polymers have become very attractive owing to their possible applications as catalysts for organic synthesis.[1] Several examples can be found of functionalized microporous polystyrenes (PSs) characterized by very low surface areas, whereby the reactive sites are accessible to the reactants only upon swelling by the solvent.[2] Swelling usually does not occur for gaseous species and this property usually prevents the use of polymer-based catalysts for gas-phase synthesis. This restriction can, however, be overcome by the use of macroporous polymeric matrices, for which a permanent open texture is obtained by 20–40% levels of cross-linking.[2] The development of easy methods to immobilize organometallic species into these polymers while maintaining their porous structure will allow their application to catalytic reactions also in the absence of a swellable solvent. An example of this class of systems is the nitrogen-containing polymers, such as poly(4-vinylpyridine) (P4VP), which play important roles as basic catalysts[3] and are used extensively to generate metal complexes with transition metals.[4]

P4VP has been used as a good support for immobilization of $CuCl_2$[5] in the oxidative carbonylation of methanol to dimethylcarbonate (DMC),[6] the oxidative coupling of 2,6-dimethylphenol,[7] and the oxidation of tetralin.[8] In these processes, all conducted in the liquid phase, Cu^{II} is reduced to Cu^{I} and HCl is released. Even though it is usually accepted that the basic N atoms of the pyridine (Py) rings act as preferential sites for Cu^{II} grafting and several models have been proposed,[4,8] there is no direct proof of the structure of the active species during the redox process. In this work, $CuCl_2$ was molecularly immobilized inside a highly cross-linked P4VP matrix characterized by permanent porosity (Figure S1 in the Supporting Information);[9] this system allowed catalysis also in the gas phase, and has been investigated in detail by in situ spectroscopy. The grafting procedure and the redox processes involving the Cu sites were investigated by means of several complementary in situ techniques (FTIR, UV/Vis, XANES, and EXAFS spectroscopy), allowing the determination of the structure of the system at each step. The determination of the structure surrounding Cu sites has to be considered a nontrivial result because of the amorphous nature of the host matrix. Detailed knowledge of the structural changes upon redox reaction is necessary for understanding more complex catalytic processes.

$CuCl_2$ coordination to the N atoms of the Py rings in P4VP matrices was demonstrated by IR spectroscopy (Figure 1): the

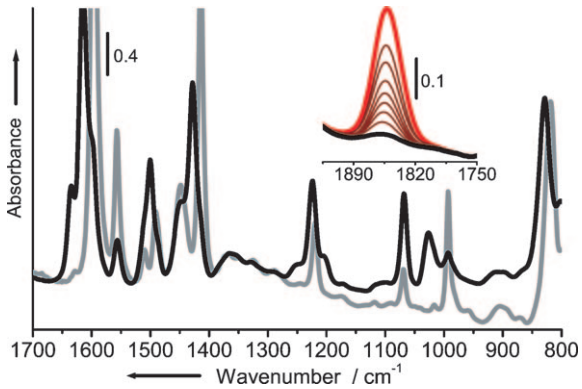

Figure 1. FTIR spectra of P4VP degassed at room temperature to remove physisorbed water before (gray) and after (black) $CuCl_2$ grafting. Inset (from black to red): NO adsorption at room temperature on the Cu^{II} sites at increasing coverage (P_{max} = 10 Torr).

coordination of Cu^{II} to the polymer, in fact, induces significant shifts in the bands characteristic of Py vibrations,[4,10] in a similar way to that observed upon coordination of strong electron-accepting molecules.[9] In particular, the bands at 1596, 1414, 993, and 818 cm^{-1} (assigned to the 8a, 19b, 1, and 11 vibrational modes of Py[9]) are most affected by Cu coordination, experiencing upward shifts of 19, 15, 33, and 10 cm^{-1}, respectively. The original P4VP bands are almost totally absent. This behavior reveals that the C–N and C–C bonds of the Py rings are strengthened as the Cu^{II} species are incorporated into the polymer,[11] and that the large majority of the Py rings are involved in the grafting procedure. Upon

[*] Dr. E. Groppo, M. J. Uddin, Prof. Dr. S. Bordiga, Prof. A. Zecchina, Prof. Dr. C. Lamberti
Department of Inorganic, Physical and Material Chemistry
NIS Centre of Excellence, and INSTM Unità di Torino
University of Torino, via P. Giuria 7, 10125 Torino (Italy)
Fax: (+39) 011-670-7855
E-mail: elena.groppo@unito.it
carlo.lamberti@unito.it

[**] C. Prestipino and G. Agostini are acknowledged for their friendly help during the XAS measurements. M. Clerici is acknowledged for constructive discussion. This work is supported by Regione Piemonte, Progetto NANOMAT Docup (2000–2006) and by Compagnia di S. Paolo. P4VP = poly(4-vinylpyridine).

Supporting information for this article is available on the WWW under http://dx.doi.org/10.1002/anie.200802815.

degassing at room temperature, physisorbed H_2O is removed (Figure S2 in the Supporting Information; note that there are almost no changes in the FTIR bands of the polymer, demonstrating that P4VP is functionalized already in the impregnation stage). Upon removal of H_2O, the grafted Cu^{II} species become accessible to NO probes, giving rise to a band at 1852 cm^{-1}, which is easily reversible upon degassing at room temperature (inset in Figure 1). The slightly lower frequency of the $\tilde{\nu}$(NO) band with respect to that observed for Cu^{II} isolated in zeolitic materials and supported on oxides[12] is indicative of higher back donation owing to the basic N ligands.

The electronic properties of the grafted $CuCl_2$ species before and after degassing at room temperature were investigated by DR (diffuse reflectance), UV/Vis, and XANES spectroscopy (Figure 2a). The as-prepared sample (inset)

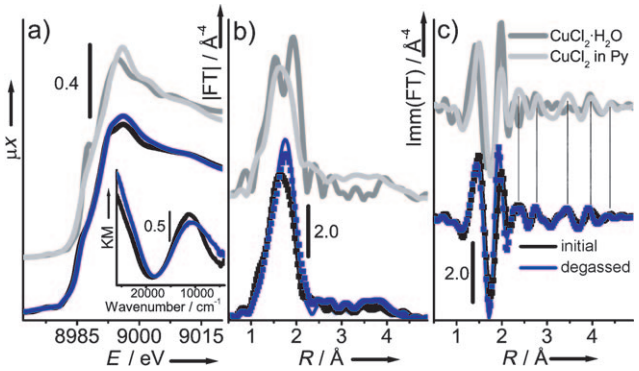

Figure 2. a) XANES and UV/Vis (inset) spectra to study the electronic properties of the grafted Cu^{II} sites. Top spectra: model compounds of bulk $CuCl_2{\cdot}2H_2O$ (dark gray) and $CuCl_2$ in Py (light gray). Bottom spectra: $CuCl_2$/P4VP sample before (black) and after (blue) dehydration at room temperature; b,c) k^3-weighted, phase uncorrected, FT of the EXAFS spectra, for both the modulus (b) and imaginary parts (c). Colors as for part (a). For the lower spectra, the experimental data (lines) are superimposed on the best fits (scattered squares). Vertical lines in part (c) show that the high-*R* signal of the $CuCl_2$/P4VP samples is the same as that of $CuCl_2$ in Py (but less intense).

shows the d–d transition typical of Cu^{II} (d^9) in pseudo-octahedral geometry. This band red shifts slightly upon removal of H_2O owing to the decreased ligand field, as already well documented in the case of isolated Cu^{II} species inside zeolitic materials.[13] The XANES spectra of the same samples (Figure 2a) are consistent with the UV/Vis spectra, showing the dipole-forbidden 1s→3d transition (weak band at 8978 eV) and the dipole-allowed 1s→4p transition (shoulder around 8986 eV).[12c,f,14–16] The main change upon dehydration is a small reduction of the white-line (first resonance after the edge) intensity, confirming a decrease in coordination number (H_2O removal). Both spectra are very similar to that of $CuCl_2$ in Py (both in the edge and white-line region) and differ from that of bulk $CuCl_2{\cdot}2H_2O$ (dark gray), which is better resolved.[17] This result indicates that Cu^{II} sites are atomically dispersed in the P4VP matrix (thus acting as a "solid solvent") and excludes the presence of clustered $CuCl_2$ species.

IR, UV/Vis, and XANES spectroscopy demonstrate that $CuCl_2$ is grafted to the Py rings of the P4VP matrix and that, upon degassing at room temperature, the Cu^{II} sites present at least one available coordination vacancy. Molecular models suggest that intermolecular coordination involving two Py moieties belonging to two different polymeric chains should occur in the P4VP matrix.[10c] However, obtaining direct structural information about the structure adopted by a metal complex inside a noncrystalline polymer is not a simple task, because X-ray diffraction is completely ineffective. Conversely, EXAFS, being selective towards the local environment of a specific absorbing atom, is well suited to give information about the local structure of Cu sites inside the amorphous P4VP matrix. The high quality of the raw EXAFS data is evident in Figure S4 in the Supporting Information. The plots of |FT| of the k^3-weighted $\chi(k)$ functions for the $CuCl_2$/P4VP sample before and after dehydration (Figure 2b) are dominated by an intense peak centered around 1.7 Å attributable to the overlapping contributions of N (from Py), Cl, and O (from H_2O, in the case of the hydrated sample) first-shell neighboring atoms, followed by smaller contributions up to 5 Å from both single (SS) and multiple scattering (MS) from the N and C atoms of the Py rings. Although the signal in this region has lower intensity, the Imm(FT) plot is in phase perfectly with that of $CuCl_2$ in Py (see vertical lines in Figure 2c), proving that the molecular $CuCl_2$ units in P4VP are actually linked to the Py rings. EXAFS analysis on the as-such sample (scattered curves in Figure 2b,c, Table 1 and Figure S5 in the Supporting Information) confirms the pseudo-octahedral Cu coordination and reveals the nature, number, and distance of the ligands: about two O atoms of coordinated water molecules at 2.05 Å, about two N atoms of linked Py rings at 2.01 Å, and two Cl ions at 2.28 Å. Dehydration leaves the high-*R* signals of the Py rings unchanged, testifying that Cu^{II} is stably linked to two Py rings, but leads to an increase of the first-shell signal and displacement of its barycenter towards higher distances. The intensity increase, unexpected for ligand removal, is actually due to the disappearance of the destructive interference between Cu–O and Cu–Cl signals that are in almost complete antiphase in a large *k* range.[18] Indeed, EXAFS analysis reveals only four first-shell ligands (two N atoms and two Cl ions); the two Cl ions are closer to the Cu^{II} center (2.25 Å) than for the hydrated sample (blue curves in Figure 2b,c, Table 1, and Supporting Information).

H_2 reduction was chosen as model reaction to investigate the structural changes undergone by the Cu^{II} sites during the more complex oxidative catalytic processes. Upon treatment of the $CuCl_2$/P4VP sample with H_2 at 450 K, HCl is released with the consequent reduction of Cu^{II} to Cu^{I}. This process is demonstrated by both UV/Vis spectroscopy (inset in Figure 3a), which shows the gradual disappearance of the Cu^{II} d–d transition,[13] and XANES (Figure 3a), which shows the appearance of an intense and well defined peak at 8983 eV attributable to the dipole-allowed 1s→4p transition, which is considered a fingerprint for Cu^{I}.[12c,f,14–16,19,20] The loss of ligands around the Cu^{I} sites and the change in their local geometry is evident by looking at the FT of the k^3-weighted $\chi(k)$ functions (Figure 3b), which show a progressive decrease

Table 1: Summary of the parameters optimized by fitting the EXAFS data.[a]

Ligand	Variable	References $CuCl_2{\cdot}H_2O$[b]	$CuCl_2$ in Py[c]	Hydrated sample[c]	$CuCl_2$/P4VP Degassed at RT[c]	Reduced by H_2[c]	Reoxidized[c]
O	C.N.	2.0 ± 0.2	–	2.0 ± 0.4	–	–	3
	R [Å]	1.96 ± 0.02	–	2.04 ± 0.03	–	–	2.00 ± 0.01
	σ^2 [Å^2]	0.004 ± 0.002	–	0.009 ± 0.003	–	–	0.008 ± 0.001
Py	C.N.	–	4.0 ± 0.4	2.4	2.4 ± 0.4	1.3 ± 0.2	1.7 ± 0.2
	R [Å]	–	2.08 ± 0.01	2.03 ± 0.01	2.04 ± 0.02	1.99 ± 0.02	2.037 ± 0.01
	σ^2 [Å^2]	–	0.007 ± 0.001	0.011 ± 0.001	0.007 ± 0.002	0.007 ± 0.003	0.006 ± 0.001
Cl	C.N.	2.0 ± 0.2	2.0 ± 0.1	2.0	2.0	1.3 ± 0.2	1.3
	R [Å]	2.29 ± 0.01	2.334 ± 0.008	2.287 ± 0.004	2.267 ± 0.009	2.149 ± 0.007	2.298 ± 0.006
	σ^2 [Å^2]	0.004 ± 0.001	0.007 ± 0.001	0.008 ± 0.001	0.005 ± 0.001	0.007 ± 0.001	0.0044 ± 0.0005
	ΔE [eV]	1 ± 1	2 ± 1	2 ± 1	2 ± 2	0	1 ± 1
	no. of variables	6	6	8	6	6	8
	R factor	0.017	0.029	0.007	0.046	0.039	0.007

[a] Coordination numbers (C.N.), distances (R), Debye–Waller factors (σ^2), and energy shift (ΔE). Non-optimized parameters are recognizable by the absence of corresponding uncertainty values. All the fits were performed in R space, over the k^3-weighted FT of the $\chi(k)$ functions calculated in the range $\Delta k = 2$–13 Å^{-1}. See the Supporting Information for more details. [b] Fit range: $\Delta R = 1.0$–2.4 Å; number of independent points: $N_{ind} = 2\Delta k \Delta R/\pi > 9$. [c] Fit range: $\Delta R = 1.1$–5.0 Å; $N_{ind} > 27$.

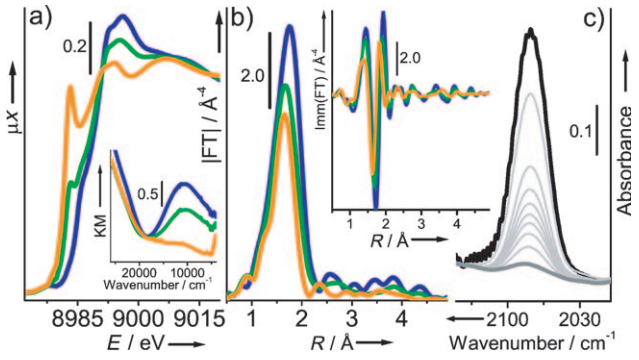

Figure 3. a) Effect of degassing at room temperature (blue) and progressive reduction in H_2 at 450 K (green and orange) of the $CuCl_2$/P4VP sample, as monitored by XANES (main part) and UV/Vis (inset) spectroscopy; b) k^3-weighted, phase-uncorrected FT of the EXAFS spectra, for both modulus (main part) and imaginary parts (inset). c) CO adsorption at room temperature on the Cu^I sites at increasing coverage ($P_{max} = 50$ Torr, black), as monitored by FTIR spectroscopy.

of the first-shell signal, accompanied by a shift toward lower distances, and the disappearance of the higher-R contributions due to MS involving the Py rings. EXAFS analysis (Table 1 and the Supporting Information) demonstrates that, on average, the Cu^I sites are linked to only one Py ring (at 1.99 Å) and one Cl ion (at 2.15 Å); the lower coordination number of the Cu^I species is responsible for the contraction of the first-shell distances. By losing a Py ligand, the Cu sites are no longer forced to stay in the plane of the remaining Py ring and acquire more degrees of freedom, resulting in heterogeneity of the angle between the N–Cu bond and the plane of the Py ring (see the two model structures in the orange box in Scheme 1). This situation implies a spread of all high-shell SS and MS paths that kill the high-R signal. Notwithstanding the low coordination number, at room temperature the so-obtained Cu^I sites are able to form only monocarbonyl complexes, characterized by the band $\tilde{\nu}(CO) = 2078$ cm^{-1} (Figure 3c). The extremely low frequency ($\Delta\tilde{\nu} = -65$ cm^{-1} vs. $\Delta\tilde{\nu} \approx +15$ cm^{-1} for $[Cu^I(CO)]$ adducts in several zeolites,[12c,d,14a,16,19,20] and $\Delta\tilde{\nu}$ between +5 and −15 cm^{-1} for CuCl and Cu_2O dispersed on oxides[12d,e,21]) reflects the high electron donation from Py to Cu^I, which reduces the electrostatic contribution and increases the π back donation in the Cu^I–CO bond.[22] The absence of polycarbonyl adducts and the easy reversibility of formation of the $[Cu^I(CO)]$ species upon degassing at room temperature suggest that, despite the apparent low coordination number determined by EXAFS, the Cu^I sites are surrounded by additional weak ligands (not ordered Py rings) that compete for the accessible coordination vacancies.

Notwithstanding the great electronic and structural changes that occur upon H_2 reduction, the Cu sites preserve their atomic dispersion, and no clustering or further $Cu^I \rightarrow Cu^0$

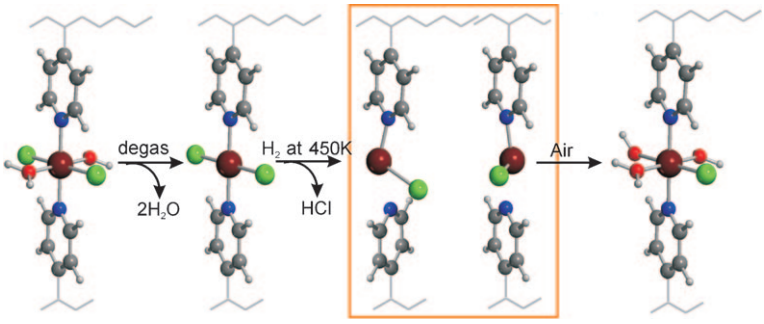

Scheme 1. Representation of the Cu environment for the stages of grafting, dehydration, reduction, and reoxidation described in the text. Cu dark red, Cl green, N blue, O red, C dark gray, H white. In the orange box only two of the many possible structures differing in N-Cu-Cl angle, which are indistinguishable by EXAFS, are represented.

reduction processes are observed, as testified by the absence of both a Cu^0 signal in the XANES spectra and Cu–Cu contributions in the EXAFS spectrum (within the sensitivity of the techniques, which is 5–10%). The reversibility of the process upon exposure of the reduced $CuCl_2$/P4VP sample to air (Figure S3 in the Supporting Information) gives the final picture. Both UV/Vis and XANES spectra (Figure S3a) testify to the occurrence of the reverse $Cu^I \rightarrow Cu^{II}$ oxidation reaction, as already demonstrated in the case of Cu^I in zeolitic frameworks.[13,15b,23] Moreover, EXAFS spectra(Figure S3 b,c) show the reappearance of the high-*R* contributions of MS from the Py rings, demonstrating that Cu^{II} sites find again the Py ligand "lost" upon reduction. From a fit of the EXAFS data, it is inferred that the Cu^{II} cations regain a pseudo-octahedral coordination geometry involving two N atoms from the Py ligands, one Cl ion, and three O atoms (either from physisorbed water molecules or from an oxidryl group, see latter part of Scheme 1). All the ligands are at almost the same distances as in the initial sample, demonstrating once again that the reduction process does not affect the nuclearity of the Cu sites.

In conclusion, the use of several complementary techniques allowed the study of the electronic and structural changes undergone by Cu sites grafted inside an amorphous nanoporous P4VP matrix during all steps of a simple redox process (as shown in Scheme 1). Even though H_2 reduction and O_2/H_2O reoxidation is a simple redox process, it well represents the more complex processes that occur during liquid-phase catalysis. Preliminary results obtained on a more complex redox reaction, involving ethylene in the gas phase as a reactant, are reported in the Supporting Information (Figure S6). From the complete knowledge of the structure of the Cu sites in all steps of the process, it emerges that the flexibility of the entire polymeric structure is the key factor in the reversibility of the redox process. In the absence of a swellable solvent, the accessibility of the active sites by a reactant in the gas phase is not straightforward, and a highly cross-linked polymeric matrix is necessary for a reagent to reach the Cu sites in the gas phase.

Experimental Section

$CuCl_2$/P4VP samples were prepared by impregnating commercial poly(4-vinylpyridine), 25% cross-linked with divinylbenzene (Aldrich), with an aqueous solution of $CuCl_2$, resulting into a Cu content of 7 wt%. H_2 reduction was performed under static conditions by dosing 100 Torr of H_2 at 450 K for 15 min, and then degassing at the same temperature; the procedure was repeated three times. FTIR spectra were collected on a Bruker IFS28 instrument at a 2 cm^{-1} resolution on self-supported pellets inside an IR cell that allows measurements under vacuum or in the presence of a desired pressure of gas. UV/Vis spectra were collected from powdered samples in a cell equipped with optical quartz windows on a Perkin–Elmer Lambda 19 spectrophotometer equipped with a reflectance sphere. X-ray absorption experiments on the Cu K-edge were performed in transmission mode at the BM29 beamline at the European Synchrotron Radiation Facility (ESRF), Grenoble (France). The XAS experimental setup and EXAFS data analysis are fully discussed in the Supporting Information.

Received: June 13, 2008
Published online: September 16, 2008

Keywords: copper · heterogeneous catalysis · redox chemistry · structure elucidation · X-ray absorption spectroscopy

[1] N. E. Leadbeater, M. Marco, *Chem. Rev.* **2002**, *102*, 3217–3273.
[2] a) P. Hodge, *Chem. Soc. Rev.* **1997**, *26*, 417–424; b) P. Barbaro, *Chem. Eur. J.* **2006**, *12*, 5666–5675.
[3] a) N. Acar, T. Tulun, *Eur. Polym. J.* **2001**, *37*, 1599–1605; b) R. V. Yarapathi, S. Kurva, S. Tammishetti, *Catal. Commun.* **2004**, *5*, 511–513.
[4] a) M. P. McCurdie, L. A. Belfiore, *Polymer* **1999**, *40*, 2889–2902; b) L. A. Belfiore, M. P. McCurdie, P. K. Das, *Polymer* **2001**, *42*, 9995–10006; c) K. H. Wu, Y. R. Wang, W. H. Hwu, *Polym. Degrad. Stab.* **2003**, *79*, 195–200; d) A. J. Pardey, A. D. Rojas, J. E. Yanez, P. Betancourt, C. Scott, C. Chinea, C. Urbina, D. Moronta, C. Longo, *Polyhedron* **2005**, *24*, 511–519; e) A. L. Santana, L. K. Noda, A. T. N. Pires, J. R. Bertolino, *Polym. Test.* **2004**, *23*, 839–845.
[5] I. Takahashi, H. Kojima, JP Patent 08325204, **1996**.
[6] a) F. Rivetti, U. Romano, EP Patent 534545, **1993**; b) Y. Sato, M. Kagotani, T. Yamamoto, Y. Souma, *Appl. Catal. A* **1999**, *185*, 219–226; c) Y. Sato, T. Yamamoto, Y. Souma, *Catal. Lett.* **2000**, *65*, 123–126; d) Y. Sato, M. Kagotani, Y. Souma, *J. Mol. Catal. A* **2000**, *151*, 79–85.
[7] H. C. Meinders, *J. Mol. Catal.* **1980**, *7*, 321–335.
[8] R. Galiasso Tailleur, C. J. G. Garcia, *J. Catal.* **2007**, *250*, 110–120.
[9] E. Groppo, M. J. Uddin, O. Zavorotynska, A. Damin, J. G. Vitillo, G. Spoto, A. Zecchina, *J. Phys. Chem. C* **2008**, accepted.
[10] a) L. A. Belfiore, M. P. McCurdie, E. Ueda, *Macromolecules* **1993**, *26*, 6908–6917; b) L. A. Belfiore, H. Graham, E. Ueda, *Macromolecules* **1992**, *25*, 2935–2939; c) L. A. Belfiore, A. T. N. Pires, Y. H. Wang, H. Graham, E. Ueda, *Macromolecules* **1992**, *25*, 1411–1419; d) A. M. Lyons, M. J. Vasile, E. M. Pearce, J. V. Waszczak, *Macromolecules* **1988**, *21*, 3125–3134.
[11] Belfiore and co-workers[4a,b,10] in their investigations of the vibrational and thermodynamic properties of different organometallic complexes inside P4VP systems coined the term "coordination cross-link" to refer to the reduction of polymeric chain mobility induced by the grafting of a complex with the consequent dramatic increase in the glass transition temperature T_g.
[12] a) G. Spoto, S. Bordiga, D. Scarano, A. Zecchina, *Catal. Lett.* **1992**, *13*, 39–44; b) G. Spoto, A. Zecchina, S. Bordiga, G. Ricchiardi, G. Martra, G. Leofanti, G. Petrini, *Appl. Catal. B* **1994**, *3*, 151–172; c) C. Lamberti, S. Bordiga, M. Salvalaggio, G. Spoto, A. Zecchina, F. Geobaldo, G. Vlaic, M. Bellatreccia, *J. Phys. Chem. B* **1997**, *101*, 344–360; d) S. Bordiga, C. Pazé, G. Berlier, D. Scarano, G. Spoto, A. Zecchina, C. Lamberti, *Catal. Today* **2001**, *70*, 91–105; e) G. Leofanti, A. Marsella, B. Cremaschi, M. Garilli, A. Zecchina, G. Spoto, S. Bordiga, P. Fisicaro, G. Berlier, C. Prestipino, G. Casali, C. Lamberti, *J. Catal.* **2001**, *202*, 279–295; f) C. Prestipino, G. Berlier, F. X. Llabrés i Xamena, G. Spoto, S. Bordiga, A. Zecchina, G. T. Palomino, T. Yamamoto, C. Lamberti, *Chem. Phys. Lett.* **2002**, *363*, 389–396; g) C. Lamberti, E. Groppo, G. Spoto, S. Bordiga, A. Zecchina, *Adv. Catal.* **2007**, *51*, 1–74.
[13] G. Turnes Palomino, P. Fisicaro, S. Bordiga, A. Zecchina, E. Giamello, C. Lamberti, *J. Phys. Chem. B* **2000**, *104*, 4064–4073.
[14] a) H. Yamashita, M. Matsuoka, K. Tsuji, Y. Shioya, M. Anpo, M. Che, *J. Phys. Chem.* **1996**, *100*, 397–402; b) Y. Kuroda, R. Kumashiro, M. Nagao, *Appl. Surf. Sci.* **2002**, *196*, 408–422; c) Y.

Kuroda, A. Kotani, H. Maeda, H. Moriwaki, T. Morimato, M. Nagao, *J. Chem. Soc. Faraday Trans.* **1992**, *88*, 1583 – 1590; d) A. Yamaguchi, T. Shido, Y. Inada, T. Kogure, K. Asakura, M. Nomura, Y. Iwasawa, *Catal. Lett.* **2000**, *68*, 139 – 145; e) W. J. Chun, Y. Koike, K. Ijima, K. Fujikawa, H. Ashima, M. Nomura, Y. Iwasawa, K. Asakura, *Chem. Phys. Lett.* **2007**, *433*, 345 – 349; f) M. H. Groothaert, J. A. van Bokhoven, A. A. Battiston, B. M. Weckhuysen, R. A. Schoonheydt, *J. Am. Chem. Soc.* **2003**, *125*, 7629 – 7640; g) J. G. Mesu, T. Visser, A. M. Beale, F. Soulimani, B. M. Weckhuysen, *Chem. Eur. J.* **2006**, *12*, 7167 – 7177; h) K. Kervinen, P. C. A. Bruijnincx, A. M. Beale, J. G. Mesu, G. van Koten, R. Gebbink, B. M. Weckhuysen, *J. Am. Chem. Soc.* **2006**, *128*, 3208 – 3217.

[15] C. Lamberti, C. Prestipino, F. Bonino, L. Capello, S. Bordiga, G. Spoto, A. Zecchina, S. D. Moreno, B. Cremaschi, M. Garilli, A. Marsella, D. Carmello, S. Vidotto, G. Leofanti, *Angew. Chem.* **2002**, *114*, 2447 – 2450; *Angew. Chem. Int. Ed. Engl.* **2002**, *41*, 2341 – 2344.

[16] a) F. X. Llabrés i Xamena, P. Fisicaro, G. Berlier, A. Zecchina, G. Turnes Palomino, C. Prestipino, S. Bordiga, E. Giamello, C. Lamberti, *J. Phys. Chem. B* **2003**, *107*, 7036 – 7044; b) C. Lamberti, S. Bordiga, F. Bonino, C. Prestipino, G. Berlier, L. Capello, F. D'Acapito, F. X. Llabrés i Xamena, A. Zecchina, *Phys. Chem. Chem. Phys.* **2003**, *5*, 4502 – 4509.

[17] $CuCl_2 \cdot 2H_2O$ in Py is assumed to be a model compound. The EXAFS data analysis reported in the Supporting Information indicates that Cu is surrounded by two Cl atoms (at 2.32 Å) and by four N atoms of the Py rings (at 2.07 Å). In other words, Py rings have displaced the weaker H_2O ligands.

[18] a) C. Prestipino, S. Bordiga, C. Lamberti, S. Vidotto, M. Garilli, B. Cremaschi, A. Marsella, G. Leofanti, P. Fisicaro, G. Spoto, A. Zecchina, *J. Phys. Chem. B* **2003**, *107*, 5022 – 5030; b) M. Tromp, J. A. van Bokhoven, A. M. Arink, J. H. Bitter, G. van Koten, D. C. Koningsberger, *Chem. Eur. J.* **2002**, *8*, 5667 – 5678.

[19] Y. Zhang, D. N. Briggs, E. de Smit, A. T. Bell, *J. Catal.* **2007**, *251*, 443 – 452.

[20] C. Lamberti, G. T. Palomino, S. Bordiga, G. Berlier, F. D'Acapito, A. Zecchina, *Angew. Chem.* **2000**, *112*, 2222 – 2225; *Angew. Chem. Int. Ed.* **2000**, *39*, 2138 – 2141.

[21] D. Scarano, S. Bordiga, C. Lamberti, G. Spoto, G. Ricchiardi, A. Zecchina, C. O. Arean, *Surf. Sci.* **1998**, *411*, 272 – 285.

[22] a) A. Zecchina, S. Bordiga, G. T. Palomino, D. Scarano, C. Lamberti, M. Salvalaggio, *J. Phys. Chem. B* **1999**, *103*, 3833 – 3844; b) V. Bolis, A. Barbaglia, S. Bordiga, C. Lamberti, A. Zecchina, *J. Phys. Chem. B* **2004**, *108*, 9970 – 9983; c) A. J. Lupinetti, S. H. Strauss, G. Frenking, *Prog. Inorg. Chem.* **2001**, *49*, 1 – 112.

[23] Note that the $Cu^{I} \rightarrow Cu^{II}$ oxidation occurs in presence of both O_2 and H_2O, as is the case for Cu/zeolites.[13,16a]

